

# Prospects for next generation Cosmic Microwave Background experiments

Gianfranco De Zotti<sup>1</sup>

1. INAF-Osservatorio Astronomico di Padova, Vicolo dell'Osservatorio 5, I-35122 Padova, Italy

In this lecture, after a synthetic review of measurements of CMB temperature anisotropies and of their cosmological implications, the theoretical background of CMB polarization is summarized and the concepts of the main experiments that are ongoing or are being planned are briefly described.

## 1 Introduction

Although Cosmic Microwave Background (CMB) experiments, and notably the highly successful WMAP and *Planck* space missions, have put on a solid basis the so-called standard cosmological model and have yielded very accurate determinations of its basic parameters, the information content of the CMB has not been fully exploited yet. In particular, *Planck* can be considered the definitive mission about CMB temperature anisotropies on scales  $\geq 5$  arcmin. However, the sensitivity of *Planck* to CMB polarization was not sufficient to extract all the information carried by it. To get such information we need polarization measurements one or more orders of magnitude better than *Planck*. The present Holy Grail is the detection of *B*-mode polarization that would provide a direct test of the notion of cosmological inflation, which is at the basis of the overwhelming majority of current models of the early Universe. The importance of this scientific goal has triggered a lot of ground-based, sub-orbital and space-borne projects.

The plan of this lecture is the following. Section 2 contains a synthetic review of the accurate measurements of CMB temperature anisotropies provided by the *Planck* satellite and of their cosmological implications. Section 3 deals with CMB polarization anisotropies. Section 4 gives a short description of the main ongoing or planned next generation CMB experiments. Finally, Sect. 5 summarizes the main conclusions.

## 2 CMB temperature anisotropies

### 2.1 Where do we stand?

Starting with the COBE detection of the CMB anisotropy in Smoot et al. (1992), the mapping of the primordial CMB anisotropies in temperature and polarization, produced by the WMAP and, with higher precision, by the *Planck* satellite has allowed us to characterize the initial cosmological perturbations at about the percent level.

Anisotropies are more conveniently studied in terms of multipoles, i.e. in the Legendre (for a sphere) or Fourier (on a planar surface) space. *Planck* has determined the CMB temperature power spectrum down to fundamental limits up to

multipoles  $\ell \sim 1500$  i.e. down to  $\sim 5$  arcmin angular scales (Planck Collaboration et al., 2016a). The temperature power spectrum determination has been extended up to  $\ell \sim 3000$  by higher resolution ground based experiments such as the South Pole Telescope (SPT; George et al., 2015a; Henning et al., 2018) and the Atacama Cosmology Telescope (ACT; Crites et al., 2015; Louis et al., 2017).

Remarkably, the data can be accounted for by the standard **six-parameter** cold dark matter model with a cosmological constant ( $\Lambda$ CDM model) and a power spectrum of primordial density perturbations having a simple power-law form:

$$\mathcal{P}(k) = A_s \left( \frac{k}{k_\star} \right)^{n_s - 1}, \quad (1)$$

where  $k_\star$  is a pivot scale, generally fixed to  $0.05 \text{ Mpc}^{-1}$ .

In addition to the 2 parameters characterizing the perturbation spectrum, the model includes 4 non-inflationary parameters: the Hubble constant  $H_0$ ; the baryon density  $\omega_b = h^2 \Omega_b$  (where  $h = H_0/100 \text{ km s}^{-1} \text{ Mpc}^{-1}$  and  $\Omega_b$  is the baryon density in units of the critical density),  $\omega_c = h^2 \Omega_c$  ( $\Omega_c$  being the dark matter density in units of the critical density); the optical depth due to re-ionization,  $\tau$ .

With these 6 parameters a very good fit of the temperature power spectrum is achieved. There is no statistically significant evidence compelling us to add more parameters, despite the many extensions that have been explored (Planck Collaboration et al., 2014a,b, 2016b,e).

Importantly, the model includes only the adiabatic growing mode for primordial fluctuations, as predicted for inflation driven by a single scalar field. No statistically significant evidence was uncovered showing that isocurvature modes were excited (Planck Collaboration et al., 2014b, 2016e), which is possible in multi-field inflationary models.

One of the most significant findings, first made by WMAP at modest statistical significance and later by *Planck* at much higher significance (Bennett et al., 2013), was that the primordial power spectrum is not exactly scale invariant: in other words,  $n_s \neq 1$  (Planck Collaboration et al., 2014b, 2016e). A value of  $n_s$  very close to unity would require an unnatural fine tuning.

*Planck* also set tight constraints on deviations of the statistics of primordial fluctuations from a Gaussian distribution (Planck Collaboration et al., 2014c, 2016d). These bounds rule out at high statistical significance many non-standard inflationary models predicting a level of non-Gaussianity allowed by WMAP (Bennett et al., 2013).

## 2.2 Is there room to improve over *Planck*?

To answer this question let us consider the errors on the CMB power spectra,  $C_\ell$ . If the underlying stochastic process is nearly Gaussian, as found by *Planck*, we have, approximately (Knox, 1995)

$$\left( \frac{\Delta C_\ell}{C_\ell} \right)_{\text{rms}} = \sqrt{\frac{2}{f_{\text{sky}}(2\ell + 1)} \frac{C_\ell + N_\ell}{C_\ell}}, \quad (2)$$

where  $f_{\text{sky}} = A/4\pi$  is the sky fraction surveyed ( $A$  is the solid angle covered by the survey),  $C_\ell$  is the expected or theoretical power spectrum and  $N_\ell$  is the power spectrum of the measurement noise.

In the ideal case of negligible noise ( $C_\ell \gg N_\ell$ ), the uncertainty is due to the “cosmic variance”<sup>1</sup>: we cannot further improve our determination of the power spectrum because it is a statistics of a stochastic process and we have only one realization of the sky. Thus, with regard to the determination of the power spectrum, a further decrease of  $N_\ell$  is of only marginal added value.

At high multipoles (small angular scales) the cosmic variance decreases and eventually the error becomes noise-dominated. The noise power spectrum is boosted as we reach the multipole corresponding to the angular resolution,  $\theta$ , of the instrument:  $\ell \simeq 60^\circ/\theta$ , with  $\theta$  in degrees (White et al., 1994). If the beam profile is Gaussian with full width at half maximum (FWHM)  $\theta$ , the noise is boosted exponentially:

$$N_{\ell,\text{boost}} \simeq N_\ell \exp\left(\frac{\ell^2 \theta^2}{2\sqrt{2} \ln 2}\right). \quad (3)$$

*Planck* sensitivity was so high that it was at the cosmic variance limit up to  $\ell \simeq 1500$ , i.e. up to its maximum resolution. At higher multipoles its noise blows up according to eq. (3). A higher resolution ( $\theta \sim 2'$ ) mission, with the high sensitivity allowed by modern technology, could reach the cosmic variance limit up to  $\ell \simeq 3000$  (cf. the left panel of Fig. 1 of George et al., 2015b).

Note that also ground-based experiments can reach the cosmic variance limit at high- $\ell$ 's. On the other hand, at low- $\ell$ 's a full-sky coverage, possible only from space, is necessary.

Note also that the high- $\ell$  regime corresponds to the damping tail of CMB anisotropies. The CMB signal is weak and its recovery requires a very accurate removal of foreground emission, dominated by point sources. On the other hand, high resolution surveys have a great potential to enhance our knowledge of extragalactic sources (De Zotti et al., 2015, 2018).

There is much more room for improvement on polarization measurements. Here the *Planck* noise is well above the cosmic variance limit ( $f_{\text{sky}} = 1$ ) for the *EE* power spectrum (defined in Sect. 3) except for the lowest multipoles (cf. the right-hand panel of Fig. 1 of George et al., 2015b).

As illustrated in that figure, the higher sensitivity (compared to *Planck*) provided by the modern technologies allows a substantial improvement, even without a higher resolution.

### 3 CMB polarization anisotropies

#### 3.1 The quest for information on the physics of primordial inflation

At the sensitivity level of presently available data, the initial conditions of the universe are described by just two numbers: the amplitude of primordial curvature perturbations,  $A_s$ , and its spectral index  $n_s$ . But at this level the form of the power spectrum follows from the weakly broken scaling symmetry of the inflationary space-time and is therefore rather generic.

Only upper limits are available on other quantities that can provide detailed information about the microphysical origin of inflation such as (cf. Tab. 1 of George

<sup>1</sup>It should be noted that the cosmic variance refers to  $f_{\text{sky}} = 1$ . If  $f_{\text{sky}} < 1$  we are dealing with the “sample variance” that is different for different surveyed areas.

et al., 2015b): the “running” of the spectral index of scalar perturbations i.e. its dependence on the scale of perturbations,  $dn_s/d \ln k$ ; the amplitude,  $A_t$ , and spectral index,  $n_t$ , of tensor perturbations; the tensor to scalar ratio  $r = A_t/A_s$ ; the spatial curvature,  $\Omega_k$ ; the non-Gaussianity of primordial perturbations; the amount of isocurvature perturbations, yielded by extra fields at inflation; topological defects, whose detection would be informative on the end of inflation.

With future, much higher sensitivity information, we expect much more detailed information about the physics of the inflationary era. In particular, crucial information is expected from primordial  $B$ -mode polarization, produced by tensor perturbations.

### 3.2 Physics of CMB polarization

The differential cross-section for Thomson scattering into the solid angle element  $d\Omega$  of unpolarized radiation is (Rybicki & Lightman, 1979)

$$\frac{d\sigma}{d\Omega} = \frac{1}{2} r_0^2 (1 + \cos^2 \theta), \quad (4)$$

where  $r_0 = e^2/m_e c^2 \simeq 2.82 \times 10^{-13}$  cm is the “classical electron radius” and  $\theta$  is the angle between the scattered and the incident photon. The incident light sets up oscillations of the target electron in the direction of the electric field vector  $E$ , i.e. the polarization. The scattered radiation intensity thus peaks in the direction normal to, with polarization parallel to, the incident polarization.

In the case of unpolarized isotropic radiation, the polarization induced by scattering in two perpendicular directions balance and the radiation remains unpolarized. The same happens in the case of a dipole anisotropy. But if the radiation possesses a quadrupole anisotropy the scattered radiation acquires a linear polarization. A reversal in sign of the temperature fluctuation corresponds to a  $90^\circ$  rotation of the polarization, which reflects the spin-2 nature of polarization (Hu & White, 1997).

### 3.3 $E$ and $B$ modes

Linear polarization is measured by the Stokes parameters  $Q$  and  $U$ . However, these quantities depend on an arbitrary choice of the coordinates. Under a coordinate rotation by an angle  $\phi$  they transform as:

$$\begin{pmatrix} \tilde{Q} \\ \tilde{U} \end{pmatrix} = \begin{pmatrix} \cos(2\phi) & \sin(2\phi) \\ -\sin(2\phi) & \cos(2\phi) \end{pmatrix} \begin{pmatrix} Q \\ U \end{pmatrix}. \quad (5)$$

This dependence on coordinates is not very convenient. To define a coordinate-independent quantity for the distribution of polarization patterns in the sky we need to go to Fourier space. This allows us to describe the polarization pattern by its orientation relative to itself.

There are two directions picked out by a polarization pattern: that which is picked out by its orientation and that which is picked out by its amplitude. The amplitudes of the polarization patterns are modulated in space by the plane wave they are sitting on.

We can then construct two quantities,  $E$  and  $B$  such that (Seljak, 1997; Zaldarriaga & Seljak, 1997; Kamionkowski et al., 1997):

$$Q(\theta) = \int \frac{d^2\ell}{(2\pi)^2} (E_\ell \cos(2\phi_\ell) - B_\ell \sin(2\phi_\ell)) \exp(i\ell\theta),$$

$$U(\theta) = \int \frac{d^2\ell}{(2\pi)^2} (E_\ell \sin(2\phi_\ell) + B_\ell \cos(2\phi_\ell)) \exp(i\ell\theta).$$

Following E. Komatsu<sup>2</sup> let us consider  $Q$  and  $U$  that are produced by a single Fourier mode. Taking the x-axis to be the direction of a wavevector, we obtain:

$$Q(\theta) = E_\ell \exp(i\ell\theta)$$

$$U(\theta) = B_\ell \exp(i\ell\theta).$$

Thus the  $E$ -mode is the Stokes  $Q$ , defined with respect to the wavevector as the x-axis; the  $B$ -mode is the Stokes  $U$ , defined with respect to the wavevector as the y-axis. The  $E$ -mode describes the polarization directions parallel or perpendicular to the wavevector; the  $B$ -mode describes the polarization directions tilted by  $45^\circ$  with respect to the wavevector. These definitions no longer depend on an arbitrary choice of the coordinates.

The  $E$ -mode is unchanged under a reflection (even parity), while the  $B$ -mode changes sign (odd parity). This implies that the  $EB$  and  $TB$  cross-power spectra vanish for parity-preserving fluctuations because  $EB$  and  $TB$  change sign under parity flip. In addition to the 3 auto-power spectra ( $TT$ ,  $EE$  and  $BB$ ) there is only one non vanishing temperature-polarization cross-spectrum, namely  $TE$ .

Density perturbations just generate parallel polarization and so generate only  $E$ -mode polarization. Gravitational waves generate both and so have a component of  $B$ -mode polarization<sup>3</sup>.

As the CMB radiation possesses a primary quadrupole moment, Thomson scattering between the CMB photons and free electrons generates linear polarization. This is the case both at recombination and at re-ionization. Re-scattering of the CMB photons at reionization generates a new polarization anisotropy on larger angular scales than at recombination because the horizon has grown to a much larger size by that epoch.

### 3.4 Measurements of CMB polarization and re-ionization

Measurements of the  $EE$  and  $TE$  power spectra have been obtained by several experiments: WMAP (Page et al., 2007; Nolta et al., 2009; Larson et al., 2011; Bennett et al., 2013), SPTpol (George et al., 2015a; Henning et al., 2018); ACTpol (ACT; Crites et al., 2015; Louis et al., 2017); POLARBEAR (Polarbear Collaboration et al., 2014; POLARBEAR Collaboration et al., 2017); BICEP/Keck Array (Barkats et al., 2014), among others. The most accurate determinations have been provided by the *Planck* mission (Planck Collaboration et al., 2016a).

A very important information provided by these power spectra is about the cosmic re-ionization. The location of the anisotropy peak in the CMB power spectrum

<sup>2</sup>Lectures given at the XIII School of Cosmology November 12–18, 2017, Cargèse, available at [http://www.cpt.univ-mrs.fr/~cosmo/EC2017/Programme17\\_a.html](http://www.cpt.univ-mrs.fr/~cosmo/EC2017/Programme17_a.html)

<sup>3</sup><http://background.uchicago.edu/~whu/intermediate/Polarization/polar5.html>.

relates to the horizon size at the new ‘last scattering’ and thus depends on the ionization redshift  $z_{\text{reion}}$ . A fitting formula was given by Liu et al. (2001):

$$\ell_{\text{peak}} \simeq 0.74(1 + z_{\text{reion}})^{0.73} \Omega_{\text{m}}^{0.11}, \quad (6)$$

where  $\Omega_{\text{m}}$  is the matter (baryons+dark matter) density in units of the critical density. The peak amplitude is a measure of the optical depth to reionization,  $\tau$ .

The re-ionization produces a low- $\ell$  peak both in the  $EE$  and in the  $TE$  power spectra. The latter has a much larger amplitude (because the temperature fluctuations are much larger than the polarization fluctuations), allowing an early detection by WMAP. However, it is affected by a much larger cosmic variance (arising from the temperature term) and has an intrinsically weaker dependence on  $\tau$  ( $TE \propto \tau$ ,  $EE \propto \tau^2$ ); also, there is only a partial correlation between  $T$  and  $E$  (Planck Collaboration et al., 2016h).

As a consequence, the low- $\ell$   $EE$  power spectrum dominates the constraints on  $\tau$ . The latest estimate is  $\tau = 0.055 \pm 0.009$  (Planck Collaboration et al., 2016g). This largely removes the tension with constraints on  $\tau$  derived from optical/UV data, implied by earlier estimates yielding higher values of  $\tau$  (Planck Collaboration et al., 2016h).

### 3.5 $B$ -mode from gravitational lensing

The weak gravitational lensing of the CMB due to the intervening matter distribution converts  $E$ -modes to the  $B$ -modes (also generating non-zero  $TB$  and  $EB$ -correlations), in addition to smoothing the acoustic oscillations of the power spectra of temperature and  $E$ -mode anisotropies and of adding power at  $\ell \gtrsim 3000$ . This signal is totally independent from the existence of primordial  $B$  modes, i.e. of tensor modes in the early universe (see Sect. 3.6).

That due to gravitational lensing is the only  $B$ -mode signal detected so far. The signal is weak and the observed signal is affected by noise, residual foregrounds, systematics and cosmic variance. To ease the estimate of its power spectrum a successful strategy consists in cross-correlating the total observed  $B$ -mode map with a template constructed by combining a tracer of the gravitational potential and an estimate of the primordial  $E$ -modes. Cross-correlating with the cosmic infrared background (CIB), the SPTpol team (Hanson et al., 2013) reported the first estimate of the lensing  $B$ -mode power spectrum. A similar cross-correlation result was obtained by the POLARBEAR (Ade et al., 2014a) and the ACTpol (van Engelen et al., 2015) groups.

The first direct evidence for polarization  $B$ -mode based on purely CMB information was reported by the POLARBEAR collaboration (Ade et al., 2014b), using the four-point correlations of  $E$ - and  $B$ -mode polarization. An improved measurement from a blind analysis of data from the first two seasons of POLARBEAR observations was presented by POLARBEAR Collaboration et al. (2017).

Planck Collaboration et al. (2016c) detected lensing  $B$ -modes in the *Planck* data at a significance of  $10\sigma$ , using both a cross-correlation with the CIB as a tracer of the lensing potential, as well as a CMB-only approach using the  $TTEB$  trispectrum. This paper also presented a measurement of the CMB lensing potential, significant at the  $40\sigma$  level, using temperature and polarization data from the *Planck* 2015 full-mission release.

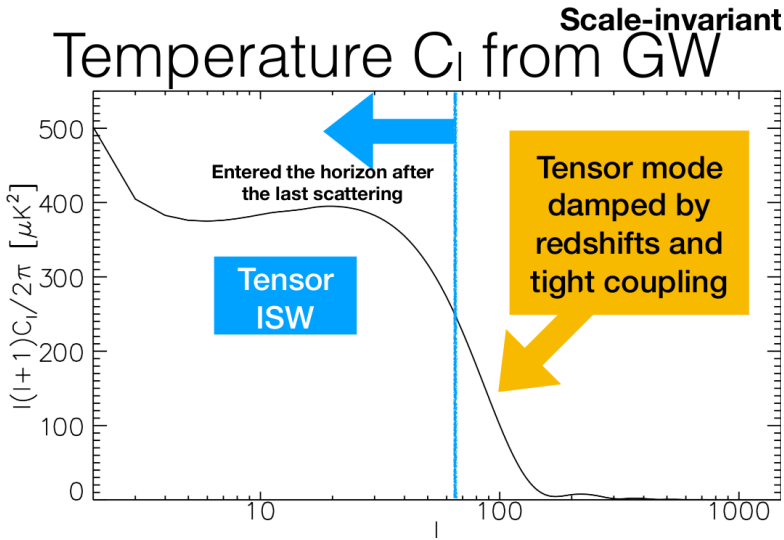


Fig. 1: Power spectrum of temperature anisotropies due to gravitational waves. Courtesy of Eiichiro Komatsu; see his lectures given at the XIII School of Cosmology November 12–18, 2017, Cargèse.

An important outcome of the determination of the lensing potential are tight constraints on the effective number of neutrino species,  $N_{\text{eff}}$ , and on the sum of neutrino masses,  $\sum m_\nu$  (for an exhaustive discussion see Abazajian et al., 2015). Combining *Planck* observations with other astrophysical data Planck Collaboration et al. (2016b) find  $N_{\text{eff}} = 3.15 \pm 0.23$  and  $\sum m_\nu < 0.23$  eV.

The constraints on  $\sum m_\nu$  imply that neutrino masses have a very weak effect on primordial CMB temperature anisotropies. Improvements on these constraints will therefore be driven primarily by accurate measurements of lensing  $B$ -modes. Next generation CMB experiments combined with improved measurements of large scale structure will have the power to detect properties of neutrinos with high accuracy, complementing the results of large laboratory experiments.

Planck Collaboration et al. (2016f) have produced a nearly all-sky template map of the lensing-induced  $B$ -modes. This map was built combining two sets of *Planck* results: the measurements of the polarization  $E$ -modes and the integrated mass distribution obtained via the reconstruction of the CMB lensing potential. It will be particularly useful for experiments searching for primordial  $B$ -modes (see Sect. 4), since it will allow an estimate of the lensing-induced contribution to the measured total CMB  $B$ -modes.

### 3.6 Primordial $B$ -modes

The simplest and canonical model for inflation, namely single-field slow-roll inflation, made a number of predictions that have been confirmed by all current cosmological data: primordial perturbations are adiabatic; the spectrum of primordial perturbations is very nearly, but not precisely, scale invariant; the distribution of primordial perturbations is very nearly Gaussian.

The model also predicts the existence of a stochastic background of gravitational waves. Their detection would constitute a fairly definitive test of the prevailing single-field slow-roll models of inflation (Kamionkowski & Kovetz, 2016). Primordial CMB  $B$ -mode polarization is the specific signature of such gravitational waves and, as such, provides direct information on the physics of primordial inflation.

In fact, density (scalar perturbations) have polarization amplitudes that change only parallel or perpendicular to the wave vector, i.e. carry only  $E$ -mode polarization (apart from the secondary effect of gravitational lensing). But gravitational waves stretch the space, creating quadrupole temperature anisotropy without velocity potential. The stretching in one direction is accompanied by a contraction in the perpendicular direction. Since the wavelength of light is also stretched, stretching/contraction results in a drop or raise of the temperature. The polarization is parallel to the hot regions and has components both parallel/perpendicular to the wave-number vector ( $E$ -mode) and tilted by  $45^\circ$  from that vector ( $B$ -mode). The two components have similar amplitude, but on small scales  $B$  is smaller than  $E$  because  $B$  vanishes on the horizon (see the lectures by E. Komatsu mentioned above).

The amplitude of inflationary tensor modes is typically expressed in terms of the tensor-to-scalar ratio  $r = A_t/A_s$ . The parameter  $r$  provides a measure of the expansion rate during inflation (Abazajian et al., 2016)

$$H_{\text{infl}} = 2.3 \times 10^{13} \left( \frac{r}{0.01} \right)^{1/2} \text{ GeV}, \quad (7)$$

which can be related to the energy scale,  $V$ , of inflation,

$$V = 1.04 \times 10^{16} \left( \frac{r}{0.01} \right)^{1/4} \text{ GeV}. \quad (8)$$

The observation of primordial tensor modes would therefore associate inflation with physics at the Grand Unified Theory (GUT) scale, estimated to be around  $10^{16}$  GeV.

The anisotropy power spectra due to tensor perturbations are induced by gravity, that is the only agent on super-horizon scales. When a perturbation enters the horizon, the cosmological expansion damps the amplitude of tensor modes via redshift. The tight coupling between electrons and photons (before recombination) also damps temperature anisotropies. Those due to tensor perturbations are not restored because gravitational waves are very weakly coupled to photons. So only anisotropies on super-horizon scales at recombination ( $\ell \gtrsim 60$ ) survive (see Fig. 1).

This limits the power of temperature anisotropies to constrain gravitational waves since the sampling variance of the dominant scalar perturbations is large at low  $\ell$ . Fortunately, CMB polarization provides an alternative route to detecting the effect of gravitational waves on the CMB which is not limited by cosmic variance of scalar perturbations since, as mentioned above, density perturbations do not produce  $B$ -modes and those due to gravitational lensing decline quickly at low multipoles.

There is no definitive prediction for the magnitude of  $r$ . However, some arguments suggest  $r \gtrsim 0.001$  (Kamionkowski & Kovetz, 2016). Models currently of special interest (e.g., Starobinsky's  $R^2$  and Higgs inflation) predict  $r \sim 0.003$ . The detection of a signal at this level requires extreme sensitivity, control of systematic effects and foreground removal.

BICEP2 Collaboration et al. (2014) reported a significant ( $> 5\sigma$ ) excess of  $B$ -mode power over the  $r = 0$  lensed- $\Lambda$ CDM expectation over the multipole range

$30 < \ell < 150$ . Some ( $\simeq 1.7\sigma$ ) evidence against the possibility that the signal can be accounted for by Galactic dust emission was presented, based on the cross-spectrum against 100 GHz maps from the previous BICEP1 experiment. It was also pointed out that the detected  $B$ -mode level was in excess of that expected from several dust models.

However *Planck* observations at high Galactic latitude and, in particular in a field centered on the BICEP2 region, found a level of polarized dust emission at 353 GHz sufficient to account for the 150 GHz excess observed by BICEP2, although with relatively low signal to noise (Planck Collaboration et al., 2016i). A joint analysis of BICEP2/Keck and *Planck* data (BICEP2/Keck Collaboration et al., 2015) showed that the BICEP2/Keck 150 GHz polarization map was correlated with the *Planck* 353 GHz map of polarized dust emission, implying that the entire BICEP2  $B$ -mode excess could be attributed to dust. This left a 95% confidence upper limit  $r < 0.12$ . An improved analysis of BICEP2 and Keck Array data, including the 95 GHz band (BICEP2 Collaboration et al., 2016), has tightened the 95% upper limit to  $r < 0.09$ . Combining the BICEP2/Keck data with constraints from the *Planck* analysis of CMB temperature plus baryon acoustic oscillations and other data yielded a combined limit  $r < 0.07$ , again at the 95% confidence level; this limit is however somewhat model dependent.

## 4 Next generation CMB experiments

Several projects for next generation CMB experiments are being planned. The main goal are accurate measurements of polarization anisotropies, with emphasis on the search for primordial  $B$ -modes. However there is a renewed interest also on new measurements of the CMB spectrum. A short summary of major projects follows.

### 4.1 LiteBIRD

The **L**ite (**L**ight) satellite for the studies of **B**-mode polarization and **I**nflation from cosmic background **R**adiation **D**etection<sup>4</sup> is, since September 2016, in the Japan Aerospace Exploration Agency/Institute of Space and Astronautical Science (JAXA/ISAS) conceptual design phase, called ISAS Phase-A1.

In February 2017 it was selected as one of 28 highest-priority large projects by the Science Council of Japan and in July of the same year as one of 7 projects that should be listed in the “Roadmap 2017 on promotion of large research projects” by the Ministry of Education, Culture, Sports, Science & Technology in Japan.

The mission goal is the verification of the inflation scenario by detecting the primordial  $B$ -modes. More precisely, the mission requirements are:

- Measurement of the  $B$ -mode polarization power spectrum on large angular scales ( $2 \leq \ell \leq 200$ ).
- Measurement of the tensor to scalar ratio  $r$  with a precision  $\sigma_r < 0.001$ , without subtracting the gravitational lensing  $B$  modes.

The mission specifications are<sup>5</sup>:

---

<sup>4</sup><http://litebird.jp/>

<sup>5</sup>See [http://litebird.jp/wp-content/uploads/2012/03/LNPC\\_LiteBIRD\\_uozumi\\_small.pdf](http://litebird.jp/wp-content/uploads/2012/03/LNPC_LiteBIRD_uozumi_small.pdf) and Suzuki et al. (2018).

- Operation at the second Lagrangian point of the Earth–Moon system (L2), located at about 1.5 million km from the Earth, directly ‘behind’ it, as viewed from the Sun.
- Full sky scan.
- Optimized for large-angle measurements of the primordial  $B$ -modes. Telescope aperture size: 40 cm; beam size  $< 1^\circ$  over the full observing frequency range; field of view  $10^\circ \times 20^\circ$ .
- High detector sensitivity:  $3 \mu\text{K arcmin}$ , with margin.
- Broad frequency range (40–400 GHz, with 15 frequency bands) to characterize and remove polarized foreground emission.
- Launch around 2025–2027.
- Three years of operation.

## 4.2 CORE

The **Cosmic ORigin Explorer** (Principal Investigator: J. Delabrouille; co-leads: P. de Bernardis and F. R. Bouchet) was proposed to ESA in answer to the “M5” call for a medium-sized mission. Although it was not selected, work on this project is still ongoing in view of a resubmission at the next call.

The Executive Board includes representatives of many European countries (in alphabetical order: Austria, Belgium, Denmark, Finland, France, Germany, Ireland, Italy, Netherlands, Norway, Poland, Portugal, Spain, Switzerland, United Kingdom) as well as of the USA.

The baseline design specifications of CORE are (Delabrouille et al., 2018):

- A 1.2 m telescope.
- The instrument works at the diffraction limit, with angular resolutions ranging from  $\simeq 2'$  at the highest frequencies to  $18'$  at the lowest. Note that *Planck* did not work at the diffraction limit at its highest frequencies. This is why CORE reaches higher angular resolutions with a somewhat smaller telescope.
- The observations are made with a single integrated focal-plane instrument, consisting of an array of 2100 cryogenically-cooled, linearly-polarised detectors. The full array aggregate CMB sensitivity is about  $1.7 \mu\text{K arcmin}$ , 25 times better than *Planck*.
- There are 19 frequency channels, distributed over a broad frequency range, from 60 to 600 GHz. Frequency channels are chosen to cover a frequency range sufficient to disentangle the CMB from astrophysical foreground emission. This is essential because even at frequencies where foreground emission is the lowest relative to the CMB, to reach the wanted sensitivity to the CMB polarization, more than 99% of the Galactic emission must be removed from the observed maps, and/or the foreground emission contribution to the angular power spectrum of the observations must be modelled with  $10^{-4}$  precision. Six frequency channels ranging from 130 GHz to 220 GHz are dedicated primarily

to observing the CMB. Six channels from 60 to 115 GHz monitor low-frequency foregrounds (polarised synchrotron, but also free-free and spinning dust in intensity, and in polarization if required). Seven channels ranging from 255 to 600 GHz serve to monitor dust emission, and to map the cosmic infrared background (CIB) anisotropies that can serve as a tracer of mass for “de-lensing” CMB polarization  $B$ -modes.

- The satellite will observe the sky for 4 years from a large Lissajous orbit around the L2 point. The scanning strategy combines three rotations of the spacecraft over different timescales. In this way about 50% of the sky will be covered every few days.

Thanks to its substantially improved sensitivity and angular resolution compared to *Planck*, CORE will also provide a lot of interesting information on Galactic emissions, on extragalactic radio sources and dusty galaxies (De Zotti et al., 2018) and on galaxy clusters detected via the Sunyaev-Zeldovich effect (Melin et al., 2018).

### 4.3 PICO

The **P**robe of **I**nflation and **C**osmic **O**rigins (formerly, CMB-Probe; P.I.: S. Hanany)<sup>6</sup> is one of the 8 Probe-Scale (\$ 400M – \$ 1000 M) space missions whose study is being funded by NASA. It will conduct a millimeter/sub-millimeter wave polarimetric survey of the entire scale with:

- A 1.4 m telescope.
- 21 bands, with 25% bandwidth, covering the frequency range from 21 to 799 GHz.
- 12,356 transition edge sensor bolometers plus multiplexed readouts.

The instrument will work at the diffraction limit, with angular resolutions ranging from  $\simeq 38'$  at the lowest frequency to  $\simeq 1'$  at the highest. The sensitivity to polarization in the central (“CMB”) channels, from  $\simeq 80$  to  $\simeq 135$  GHz is  $\leq 1.7 \mu\text{K}\cdot\text{arcmin}$ . The survey will be carried out for 4 years, from L2.

Like CORE, PICO will provide a rich harvest of new data also on astrophysical foregrounds. Its  $\simeq 1'$  angular resolution at the highest frequencies is ideal to detect the sub-mm emission of proto-clusters of dusty galaxies. This will allow the investigation of early phases of cluster evolution, before the establishment of the hot intergalactic medium that makes them visible in X-rays or via the Sunyaev-Zeldovich effect.

### 4.4 CMB-S4

The CMB-Stage IV (CMB-S4; Abazajian et al., 2016; Abitbol et al., 2017) is a US-led ground based program building on Stage 2 and 3 projects. It is expected to start operating in  $\sim 2021$ . Like the projects mentioned above, it aims at investigating

---

<sup>6</sup>See <https://zzz.physics.umn.edu/groups/ipsig/cmbprobe2016proposal> and Presentations/Posters at <https://zzz.physics.umn.edu/ipsig/start?&#presentationsposters>.

primordial inflation by mapping the polarization of the CMB to nearly the cosmic variance limit for a broad range of angular scales.

It targets to deploy  $\sim 500,000$  effectively background-limited detectors, spanning the 30 to 300 GHz frequency range. Since any current single telescope design cannot admit such a large number of detectors, CMB-S4 will use an array of multiple telescopes. A conservative design of CMB-S4 would include both small and large telescopes. Small telescopes have the role of setting the most sensitive constraints on the degree scale, i.e. on the recombination peak of polarization power spectra. To this end, they can be built with entirely cryogenic optics, reducing detector noise due to optical loading from the telescope.

Large telescope, will have primary apertures in the 2–10 m diameter range, in order to achieve an optical beam size in the range of 1–4 arcminutes at  $\simeq 100 - 150$  GHz. This will allow the measurement of CMB power spectra up  $\ell_{\max} \sim 5000$ , to meet many of the science requirements including those that exploit gravitational lensing, measurements of the damping tail, and galaxy cluster measurements. In particular, the arcmin angular resolution will be optimally suited for “de-lensing”, i.e. to measure and remove the contribution to the  $B$ -mode power spectrum from gravitational lensing of CMB  $E$ -modes.

The polarization sensitivity will be of  $\sim 1 \mu\text{K arcmin}$  over  $\gtrsim 70\%$  of the sky, and better in deep fields. It is foreseen that, thanks to these performances, CMB-S4 will reach uncertainties on the tensor-to-scalar ratio  $r$ , on the effective number of neutrino species and on the sum of neutrino masses of  $\sigma(r) = 0.001$ ,  $\sigma(N_{\text{eff}}) = 0.02\text{--}0.03$  and  $\sigma(\sum m_\nu) = 20\text{--}30$  meV, respectively.

The arcmin resolution is also crucial for extragalactic science, e.g. for detecting high- $z$  strongly lensed galaxies, galaxy clusters via the Sunyaev-Zeldovich effect and galaxy proto-clusters via the mm/sub-mm emission of member galaxies. Thanks to its sensitivity and to its better resolution at mm wavelengths, CMB-S4 will detect highest redshift sources than CORE or PICO, up to  $z \gtrsim 6$ , as demonstrated by the SPT results (Marrone et al., 2018).

#### 4.5 PIXIE

The **Primordial InflaXIon** (Inflation) **Explorer** (Kogut et al., 2016) is conceptually different from all other CMB polarization missions. It is designed to measure not only polarization, but also the absolute spectrum of CMB emission, similarly to COBE-FIRAS, using a reference blackbody to which the absolute emission of the sky is compared by means of a Fourier transform spectrometer.

PIXIE covers the range from 30 to 6000 GHz in 400 frequency bands. With an overall sensitivity of about  $5 \mu\text{K-arcmin}$ , PIXIE is the least sensitive of the CMB polarization space missions considered here (about 3 times less than CORE, which directly translates into a sensitivity to the  $B$ -mode power spectrum about 9 times worse if only noise is considered). This leaves open the possibility of detecting primordial  $B$ -modes at the level  $r \sim 0.01$  with PIXIE alone.

PIXIE will also measure the CMB  $E$ -mode on the largest scales, hence can accurately determine the re-ionization optical depth  $\tau$ , but its angular resolution of about  $2^\circ.6$  is not sufficient for a clear observation of the recombination peak of inflationary  $B$ -modes, nor for any lensing or small-scale CMB  $E$ -mode science.

However, it will improve spectacularly over the COBE/FIRAS measurement of

the sky absolute brightness, allowing the detection of distortions of the CMB spectrum orders of magnitude weaker than the COBE/FIRAS upper limits. The detection of spectral distortions would have profound implications for our understanding of physical processes taking place over a vast window in the cosmological history (e.g., De Zotti et al., 2016; Chluba, 2016).

The frequency range covered by PIXIE, extending to much higher frequencies than any other CMB experiment, carries essential information about foreground emission that cannot be obtained in any other way. Particularly valuable is the accurate measurement of the CIB spectrum which is a measure of the overall energy released by dust-obscured star formation and AGN accretion, and is currently known with a  $\sim 30\%$  uncertainty.

#### 4.6 Ground-based versus space-borne CMB experiments

Large ground-based CMB programmes, like CMB-S4, can target sensitivities and angular resolutions substantially better than space-borne missions: they can operate over much longer times and use much larger telescopes.

On the other hand, they can necessarily cover a limited number of frequency bands (the main atmospheric windows are centered around minima of atmospheric emission at about 30, 90, 150, and 220 GHz) and this limits their capability of removing foreground emissions. This is a crucial point: to have foreground residuals below noise and/or cosmic variance uncertainties in bins of  $\Delta\ell \simeq 30\%$ , foreground contamination must be reduced by at least 3 orders of magnitude in amplitude at  $\ell \sim 10$ , by 2 orders of magnitude at  $\ell \sim 100$  and 1 order of magnitude at  $\ell \sim 1000$  (Delabrouille et al., 2018).

This is unlikely to be doable with ground-based experiments, which must thus exploit only the cleanest sky regions, i.e. only a limited fraction of the sky. This implies a higher sampling variance that, given the sensitivity of the planned experiments, dominates for  $\ell < 2500$  and for  $\ell < 1000$  for  $E$ - and  $B$ -modes, respectively.

Also, ground-based experiments are more liable to systematic effects. Space missions completely avoid the complexity of atmospheric absorption, emission, and fluctuations, minimise side-lobe pickup of emissions from the Earth, Sun, and Moon and fluctuations of parts of the instrument that are optically coupled to the detectors.

The history of CMB research has shown that ground-based and balloon-borne observations are essential to build technological roadmaps and for observing the small scales that are too costly from space. However, all the major steps forward have been achieved by space missions: COBE, which confirmed the blackbody spectrum of the CMB, ruling-out alternatives to the hot Big-Bang scenario, and detected the first temperature anisotropies; WMAP which set the stage for precision cosmology; *Planck* which extracted essentially all the cosmological information available in the CMB temperature spectrum on scales  $\gtrsim 5'$ .

## 5 Conclusions

The recent advances in the detector technology make possible an increase in sensitivity of CMB experiments by orders of magnitude. While *Planck* has already extracted the main cosmological information provided by CMB temperature maps, the higher sensitivity is crucial for making substantial progress on CMB polarization.

Next generation projects have the capability of measuring the CMB  $E$ -mode polarization down to the cosmic variance limit over a wide range of angular scales.

Moreover, it will be possible to push the search for primordial  $B$ -modes down to a tensor to scalar ratio  $r \sim 0.001$ . Primordial  $B$ -modes are the current Holy Grail for cosmology and fundamental physics because they provide a measure of the energy scale driving the inflation, of order of  $10^{16}$  GeV (far beyond the reach of accelerators on the ground: the maximum collision energy reached by the Large Hadron Collider at CERN is  $14 \text{ TeV} = 1.4 \times 10^{14} \text{ GeV}$ ) at  $t \sim 10^{-35}$  s.

Lensing  $B$ -modes may provide measurements of the neutrino absolute mass scale, a determination of the neutrino mass hierarchy and strong constraints on possible light relics like axions, sterile neutrinos and gravitinos.

*Acknowledgements.* I'm grateful to the organizers of the Third Cosmology School in Cracow for the kind invitation and the extraordinarily warm hospitality. Thanks are due to Eiichiro Komatsu for having provided Fig. 1. Work supported in part by ASI/INAF agreement n. 2014-024-R.1 for the *Planck* LFI Activity of Phase E2 and by the ASI/Physics Department of the university of Roma–Tor Vergata agreement n. 2016-24-H.0 for study activities of the Italian cosmology community.

## References

- Abazajian, K. N., et al., *Astroparticle Physics* **63**, 55 (2015)
- Abazajian, K. N., et al., *arXiv e-prints* (2016)
- Abitbol, M. H., et al., *arXiv e-prints* (2017)
- Ade, P. A. R., et al., *Physical Review Letters* **112**, 13, 131302 (2014a)
- Ade, P. A. R., et al., *Physical Review Letters* **113**, 2, 021301 (2014b)
- Barkats, D., et al., *ApJ* **783**, 67 (2014)
- Bennett, C. L., et al., *ApJS* **208**, 20 (2013)
- BICEP2 Collaboration, et al., *Physical Review Letters* **112**, 24, 241101 (2014)
- BICEP2 Collaboration, et al., *Physical Review Letters* **116**, 3, 031302 (2016)
- BICEP2/Keck Collaboration, et al., *Physical Review Letters* **114**, 10, 101301 (2015)
- Chluba, J., *MNRAS* **460**, 227 (2016)
- Crites, A. T., et al., *ApJ* **805**, 36 (2015)
- De Zotti, G., et al., *J. Cosmology Astropart. Phys.* **6**, 018 (2015)
- De Zotti, G., et al., *J. Cosmology Astropart. Phys.* **3**, 047 (2016)
- De Zotti, G., et al., *J. Cosmology Astropart. Phys.* **4**, 020 (2018)
- Delabrouille, J., et al., *Journal of Cosmology and Astroparticle Physics* **Issue 04**, article id. 014 (2018)
- George, E. M., et al., *ApJ* **799**, 177 (2015a)
- George, E. M., et al., *ApJ* **799**, 177 (2015b)
- Hanson, D., et al., *Physical Review Letters* **111**, 14, 141301 (2013)
- Henning, J. W., et al., *ApJ* **852**, 97 (2018)
- Hu, W., White, M., *New A* **2**, 323 (1997)
- Kamionkowski, M., Kosowsky, A., Stebbins, A., *Phys. Rev. D* **55**, 7368 (1997)

- Kamionkowski, M., Kovetz, E. D., *ARA&A* **54**, 227 (2016)
- Knox, L., *Phys. Rev. D* **52**, 4307 (1995)
- Kogut, A., et al., in Space Telescopes and Instrumentation 2016: Optical, Infrared, and Millimeter Wave, *Proc. SPIE*, volume 9904, 99040W (2016)
- Larson, D., et al., *ApJS* **192**, 16 (2011)
- Liu, G.-C., et al., *ApJ* **561**, 504 (2001)
- Louis, T., et al., *J. Cosmology Astropart. Phys.* **6**, 031 (2017)
- Marrone, D. P., et al., *Nature* **553**, 51 (2018)
- Melin, J.-B., et al., *J. Cosmology Astropart. Phys.* **4**, 019 (2018)
- Nolta, M. R., et al., *ApJS* **180**, 296 (2009)
- Page, L., et al., *ApJS* **170**, 335 (2007)
- Planck Collaboration, et al., *A&A* **571**, A16 (2014a)
- Planck Collaboration, et al., *A&A* **571**, A22 (2014b)
- Planck Collaboration, et al., *A&A* **571**, A24 (2014c)
- Planck Collaboration, et al., *A&A* **594**, A11 (2016a)
- Planck Collaboration, et al., *A&A* **594**, A13 (2016b)
- Planck Collaboration, et al., *A&A* **594**, A15 (2016c)
- Planck Collaboration, et al., *A&A* **594**, A17 (2016d)
- Planck Collaboration, et al., *A&A* **594**, A20 (2016e)
- Planck Collaboration, et al., *A&A* **596**, A102 (2016f)
- Planck Collaboration, et al., *A&A* **596**, A107 (2016g)
- Planck Collaboration, et al., *A&A* **596**, A108 (2016h)
- Planck Collaboration, et al., *A&A* **586**, A133 (2016i)
- Polarbear Collaboration, et al., *ApJ* **794**, 171 (2014)
- POLARBEAR Collaboration, et al., *ApJ* **848**, 121 (2017)
- Rybicki, G. B., Lightman, A. P., *Astronomy Quarterly* **3**, 199 (1979)
- Seljak, U., *ApJ* **482**, 6 (1997)
- Smoot, G. F., et al., *ApJL* **396**, L1 (1992)
- Suzuki, A., et al., *Journal of Low Temperature Physics* **193**, 1048 (2018)
- van Engelen, A., et al., *ApJ* **808**, 7 (2015)
- White, M., Scott, D., Silk, J., *ARA&A* **32**, 319 (1994)
- Zaldarriaga, M., Seljak, U., *Phys. Rev. D* **55**, 1830 (1997)